

Computational Studies of Bridging Structures and Isomerism in Substituted Disilynes

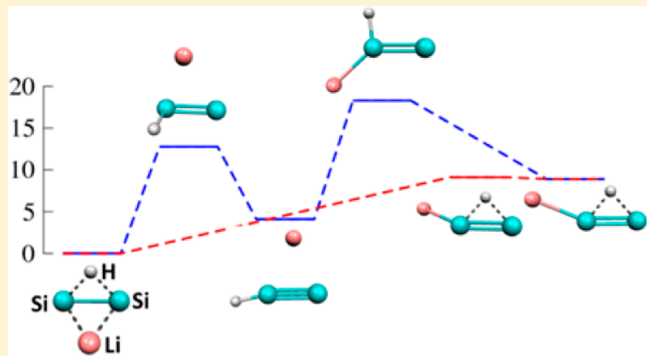
Lukasz M. Serafin,^{†,‡,§} Mark M. Law,^{‡,*} and Tanja van Mourik^{†,*}

[†]EaStCHEM School of Chemistry, University of St. Andrews, North Haugh, St. Andrews, Fife KY16 9ST, Scotland, United Kingdom

[‡]Chemistry Department, University of Aberdeen, Meston Walk, Aberdeen, AB24 3UE, Scotland, United Kingdom

Supporting Information

ABSTRACT: The substituted disilyne molecules, Si_2Li_2 and Si_2HX , where $\text{X} = \text{Li}, \text{F}$, and Cl , have been investigated using the high-level CCSD(T) and CCSD(T)-F12 *ab initio* methods. The calculations have found or confirmed the existence of several isomeric forms and transition states for each molecule. Optimized geometries, relative energies, and harmonic vibration frequencies are reported. Bridging structures exist in all cases. Comparisons are made with existing literature results for the related Si_2H_2 , C_2X_2 , and C_2HX isomerizing systems. Additionally, CCSD(T) and CCSD(T)-F12 calculations were performed for Si_2H_2 , for which experimental spectroscopic data are available. Results calculated with CCSD(T)-F12 and the cc-pVTZ-F12 basis set are of comparable quality as those computed with CCSD(T) and the much larger cc-pV(6+d)Z basis set, at much less computational cost. We recommend the CCSD(T)-F12/cc-pVTZ-F12 level of theory as a very attractive alternative to conventional CCSD(T).



1. INTRODUCTION

Four-atomic molecules of the form Si_2XY where X and $\text{Y} = \text{H}$, Li , F , or Cl , for example, are important prototypes in the study of chemical bonding generally and in the pursuit of multiply bonded silicon species in particular. The “simplest” molecule of this form, Si_2H_2 , has been studied over a long period experimentally and theoretically, but much less is known about the substituted systems. Comparisons with the isovalent C_2XY and CSiXY molecules and other heavier group 14 analogues (Ge, Sn, and Pb) are also of great current interest.

The Si_2H_2 potential energy surface differs significantly from that of C_2H_2 . C_2H_2 forms two isomers: the linear triply bonded acetylene, $\text{HC}\equiv\text{CH}$, and a doubly bonded vinylidene structure, $\text{H}_2\text{C}=\text{C}$. CCSDT calculations extrapolated to the full configuration interaction/complete basis set (FCI/CBS) limit show that $\text{HC}\equiv\text{CH}$ is more stable than $\text{H}_2\text{C}=\text{C}$ by 45 kcal/mol, whereas the (classical) isomerization barrier from $\text{H}_2\text{C}=\text{C}$ to $\text{HC}\equiv\text{CH}$ was calculated to be 2.8 kcal/mol.¹ Si_2H_2 , on the other hand, possesses four isomeric forms differing in energy by only 18 kcal/mol (at the CCSD(T) level and on the lowest singlet electronic state) and with barriers to isomerization for the metastable forms all in the range 3–5 kcal/mol. In decreasing order of stability, the isomers are dibridged, $\text{Si}(\text{H}_2)\text{Si}$; monobridged, $\text{Si}(\text{H})\text{SiH}$; disilavinyldene, H_2SiSiH ; and trans-bent, HSiSiH .² Lein et al.³ have shown that the unusual structures of E_2H_2 ($\text{E} = \text{Si-Pb}$) can be explained by considering the interactions between the EH moieties in the electronic ground state ($\text{X}^2\Pi$). Whereas C_2H_2 is bound through interactions between CH moieties in the $a^4\Sigma^-$ excited state

(resulting in the linear triply bonded acetylene structure), in the heavier homologues bonding between two $\text{X}^2\Pi$ EH fragments is favored over bonding in the excited state, because the EH excitation energy is much larger compared to that of CH. This leads to favorable dibridged, monobridged, and trans-bent structures. The unusual structures of the Si_2H_2 isomers have made this system a key target for structure and bonding and dynamics studies^{3–5} and stimulated interest in its ionic variants,⁶ and other main-group and transition metal analogues. Isomers of Si_2H_2 are also being studied in transition metal complexes^{7,8} and adsorbed on surfaces.⁹

Substitution of one or both hydrogens in C_2H_2 gives rise to a wide range of behaviors.¹⁰ For C_2HF and C_2HCl , linear and vinylidene-like isomers also occur with relative energies and isomerization barriers for H migration from the vinyl forms similar to those for C_2H_2 (45 and 2 kcal/mol for C_2HF at the CCSD(T) level¹¹ and 45 and 1 kcal/mol for C_2HCl at the QCISD(T)//MP2 level¹²). The barriers for F and Cl atom migrations are significantly larger: 47 and 13 kcal/mol, respectively.^{11,12} In contrast, only a single linear isomer has been found for C_2HLi ,¹³ while in the case of C_2Li_2 , the linear isomer lies 9 kcal/mol above the planar dibridged global minimum at the MP2/cc-pVQZ//MP2/cc-pVQZ level.¹⁴

The Si analogues of these compounds are much less well characterized. Bei and Feng optimized some isomeric structures of Si_2HX where $\text{X} = \text{Li}, \text{F}$, and Cl at the HF/6-31G** level,¹⁵

Received: April 19, 2013

Published: April 24, 2013

but as far as we are aware, there are no geometry optimizations including electron correlation. At the MP2/cc-pVQZ level, Si_2Li_2 has a dibridged minimum structure and (2 kcal/mol higher in energy) a planar dibridged transition state analogous to Si_2H_2 .¹⁶ A linear second-order saddle point, LiSiSiLi (only), has been optimized at the MP2/6-311+G(3df) level.¹⁷

In addition to the experimentally very-well-known acetylene/vinylidene system and the observed two isomers of Si_2H_2 mentioned above, four of the other molecules considered here have been detected experimentally: HCCF,¹⁸ HCCl ,¹⁹ HCCLi ,²⁰ and Si_2Li_2 .²¹

2. METHODOLOGY

Unless otherwise noted, all calculations reported here were performed with the Molpro software package²² on the EaStCHEM Research Computing Facility at the University of St. Andrews. For the geometry optimizations, starting structures were generated by taking the four Si_2H_2 isomers (dibridged, monobridged, vinylidene, and trans-bent), replacing one of the hydrogens by a Li, F, or Cl atom or both hydrogens with Li atoms, and adjusting the relevant bond lengths. The structures were optimized using the coupled cluster method with single, double, and perturbative triple excitations [CCSD(T)^{23–25}] and the aug-cc-pVTZ^{26,27} basis set, using the frozen-core approximation. Harmonic vibrational frequencies were calculated at the same level of theory. The frequency calculations employed the average isotope masses of the atoms involved (which is the default in Molpro). A number of transition state structures were located as well. The bond orders of the structures shown in the figures below were estimated based on Natural Bond Orbital (NBO)^{28,29} analysis of the HF/aug-cc-pVTZ wave functions (computed at the CCSD(T)/aug-cc-pVTZ optimized geometries) using NBO 3.1³⁰ as implemented in Gaussian 09.³¹ The structures of the minima were also optimized using CCSD(T) with the aug-cc-pVQZ basis set as well as with the explicitly correlated CCSD(T)-F12a method^{32,33} and the cc-pVTZ-F12 basis set.^{34,35} The 3C(FIX) approximation,^{36,37} which is the default in Molpro 2010.1, was employed in the preliminary density-fitting MP2-F12 computations. In the following, CCSD(T)-F12 refers to the CCSD(T)-F12a method. The cc-pVnZ-F12 ($n = 2–4$)³⁵ orbital basis set was combined with the OptRI auxiliary basis set,³⁸ which is necessary for the complementary auxiliary orbital basis (CABS) resolution of the identity step.³⁹ For Si_2HF and Si_2HCl , the aug-cc-pVnZ/JKFIT ($X = 2–4$) basis sets of Weigend⁴⁰ were used for density fitting of the Fock and exchange matrices. Because no aug-cc-pVTZ/JKFIT basis set exists for Li, the calculations on the Si_2HLi and Si_2Li_2 systems employed the def2-QZVPP/JKFIT basis set⁴¹ instead for density fitting of the Fock and exchange matrices for H, Li, and Si. Density fitting of the remaining integral quantities employed the aug-cc-pVnZ/MP2FIT ($n = 2–4$) basis sets of Weigend et al.⁴² The approximation 3C(FIX)^{32,33,43} for the diagonal fixed amplitude ansatz was employed in the preliminary density fitting MP2-F12 computations. The geminal Slater exponent value of $\beta = 1$ for the cc-VnZ-F12 ($n = 2–4$) basis sets was employed here. The triples energy was automatically scaled³³ by setting the option SCALE_TRIP=1 as suggested in the MOLPRO manual in all calculations performed here.

We also optimized the structures of the four Si_2H_2 isomers (the C_{2v} -symmetric dibridged, C_s -symmetric monobridged, C_{2v} -symmetric disilavinyldene, and C_{2h} -symmetric trans-bent isomers) with CCSD(T)/aug-cc-pVnZ and CCSD(T)-F12/

cc-pVnZ-F12 ($n = D, T, Q$). Harmonic vibrational frequencies were calculated with CCSD(T)-F12/cc-pVTZ-F12. As experimental results are available for the dibridged and monobridged Si_2H_2 isomers, these results allow us to assess the accuracy of the methods employed.

Below the aug-cc-pVnZ, cc-pVnZ-F12, and cc-pV(n+d)Z basis sets will be abbreviated as aVnZ, VnZ-F12, and V(n+d)Z, respectively.

3. RESULTS AND DISCUSSION

3.1. Si_2H_2 . Table 1 lists the equilibrium geometrical parameters of the four Si_2H_2 isomers computed with CCSD-

Table 1. Equilibrium Geometries for Isomers of Disilane Computed at Different Levels of Theory (Distances in Å; Angles in deg)

	CCSD(T)/ cc-pV(6+d)Z ^a	CCSD(T)- F12a/VTZ- F12	CCSD(T)- F12a/VQZ- F12	expt ^b
dibridged				
Si–Si	2.2067	2.2073	2.2061	2.1990
Si–H	1.6674	1.6675	1.6679	1.6637
$\tau(\text{HSiSiH})$	104.13	104.15	104.06	104.06
monobridged				
Si–Si	2.1174	2.1182	2.1170	2.119
Si ₁ –H _t	1.4871	1.4976	1.4872	1.506
Si ₁ –H _b	1.6328	1.6334	1.6332	1.586
$\angle \text{Si}_2\text{Si}_1\text{H}_t$	159.34	159.26	159.45	153.9
$\angle \text{Si}_2\text{Si}_1\text{H}_b$	52.34	52.31	52.38	52.2
vinylic				
Si–Si	2.2047	2.2056	2.2047	
Si–H	1.4818	1.4822	1.4818	
$\angle \text{SiSiH}$	123.58	123.58	123.57	
trans				
Si–Si	2.1069	2.1073	2.1064	
Si–H	1.4870	1.4872	1.4870	
$\angle \text{SiSiH}$	124.77	124.79	124.82	

^aValues taken from ref 4. ^bDibridged isomer: “Semi-experimental” equilibrium geometry derived in ref 4 from the experimental data of ref 44. Monobridged isomer: experimental ground state geometry.⁴⁵

(T)-F12 and the VTZ-F12 and VQZ-F12 basis sets. Also shown are the CCSD(T)/V(6+d)Z results of ref 4, as well as the “semi-experimental” equilibrium geometry of the dibridged isomer^{4,44} and the experimental ground state geometry of the monobridged isomer.⁴⁵ Note the very close agreement between the results obtained with CCSD(T)/V(6+d)Z and CCSD(T)-F12/VTZ-F12 as well as the good agreement with the experimental results. The excellent agreement between the CCSD(T)-F12/VTZ-F12 geometrical parameters and CCSD(T) results obtained with larger basis sets is due to the much faster convergence of CCSD(T)-F12 results with increasing basis set size. Figures S1–S3 (Supporting Information) show the variation with increasing basis set size of the Si–Si and Si–H distances and the $\tau(\text{HSiSiH})$ torsion angle of the dibridged Si_2H_2 isomer computed with CCSD(T)/aVnZ, CCSD(T)-F12/VnZ-F12 ($n = D, T, Q$), and CCSD(T)/V(n+d)Z ($n = D$ to 6). The plots clearly show that even with the VTZ-F12 basis set, the geometrical parameters computed with CCSD(T)-F12 are of similar or better quality than the CCSD(T)/V(5+d)Z results. This is in agreement with earlier observations that CCSD(T)-F12 calculations with basis sets of TZ-quality are more accurate than standard CCSD(T) calculations with 5Z-

quality basis sets.^{32,33} Note, however, that the VnZ-F12 basis sets contain more basis functions than the corresponding VnZ basis sets. For Si₂H₂, the VTZ-F12 basis set is almost as large (in terms of number of contracted basis functions) as VQZ (VTZ-F12: 7s7p4d2f/4s3p1d for Si/H, 160 basis functions for Si₂H₂; VTZ: 5s4p2d1f/3s2p1d, 86 basis functions; VQZ: 6s5p3d2f1g/4s3p2d1f, 178 basis functions). Nevertheless, the price/performance ratio of CCSD(T)-F12/cc-VnZ-F12 is striking. Figures S1 and S2 show that the Si–Si and Si–H bond distances calculated with the three different basis set series converge to a value slightly above the experimental result. This is predominantly due to the absence of core–core and core–valence correlation in the current calculations. Earlier work showed that core correlation, calculated with CCSD(T) and the cc-pCVQZ basis set, reduces the Si–Si and (terminal) Si–H bond distances in Si₂H₂ by ~0.01 and 0.0035 Å, respectively.⁴ Thus, inclusion of core correlation would bring the Si–Si and Si–H distances calculated with CCSD(T)-F12/cc-pVnZ-F12 in even better agreement with the experimental results.

The fast convergence of the CCSD(T)-F12 results is also evident from the basis set dependence of the energies (relative to the dibridged global minimum) of the monobridged, disilavinyldene, and trans-bent isomers (Supporting Information, Tables S4–S6).

Table 2 compares the harmonic vibrational frequencies of the dibridged Si₂H₂ isomer, calculated at the CCSD(T)/aVTZ,

Table 2. Calculated and Experimental Harmonic Frequencies (in cm⁻¹) for the Dibridged Si₂H₂ Isomer

CCSD(T)-F12a/ VTZ-F12	CCSD(T)/AVTZ ^a	CCSD(T)/ V(Q+d)Z ^a	semi-expt. ^b
1650	1631	1649	
1562	1544	1560	1552
1236	1221	1239	1226
1167	1152	1170	
921	909	918	922
529	515	528	

^aValues taken from ref 4. Note that the frequency calculations in ref 4 employed the isotopic masses of ²⁸Si and ¹H, whereas the CCSD(T)-F12a/VTZ-F12 calculations used the average atomic masses. The different choice of atomic masses affects the frequency values by at most 1 cm⁻¹. ^bThe “experimental” frequencies were derived in ref 4 from the experimental data of refs 58 and 59.

CCSD(T)/V(Q+d)Z, and CCSD(T)-F12/VTZ-F12 levels, with available experimental results. The CCSD(T)/aVTZ values are consistently lower than the CCSD(T)/V(Q+d)Z and CCSD(T)-F12/VTZ-F12 results, which correlates with the larger Si–Si and Si–H bond lengths calculated at this level of theory.⁴ The CCSD(T)/V(Q+d)Z and CCSD(T)-F12/VTZ-F12 frequencies are very close to each other. All three levels of theory predict the frequencies with similar accuracy. Thus, CCSD(T)-F12/VTZ-F12 appears to be an appropriate method for calculating vibrational frequencies. The CCSD(T)-F12/cc-pVTZ-F12 level of theory manifests itself as a very attractive and cost-effective alternative to conventional CCSD(T) calculations.

The CCSD(T) and CCSD(T)-F12 calculations discussed above for Si₂H₂ were not all performed on the same computer, so comparison of CPU times is not possible. However, for the remaining calculations to be discussed below we can give some representative timings: for the Si₂HLi dibridged isomer (*C*₂

symmetry), a CCSD(T)/aVTZ single-point calculation (with 169 contracted basis functions) took 65 s (CPU time) on a 12-core 2.93 GHz Intel Westmere node, a CCSD(T)/aVQZ calculation (with 294 basis functions) took 575 s while a CCSD(T)-F12/VTZ-F12 calculation (with 195 basis functions) took 95 s.

3.2. Si₂HX (X = F, Cl, Li) and Si₂Li₂. The structures of the Si₂HF, Si₂HCl, Si₂HLi, and Si₂Li₂ minima and transition states are shown in Figures 1–4, respectively. The single, double,

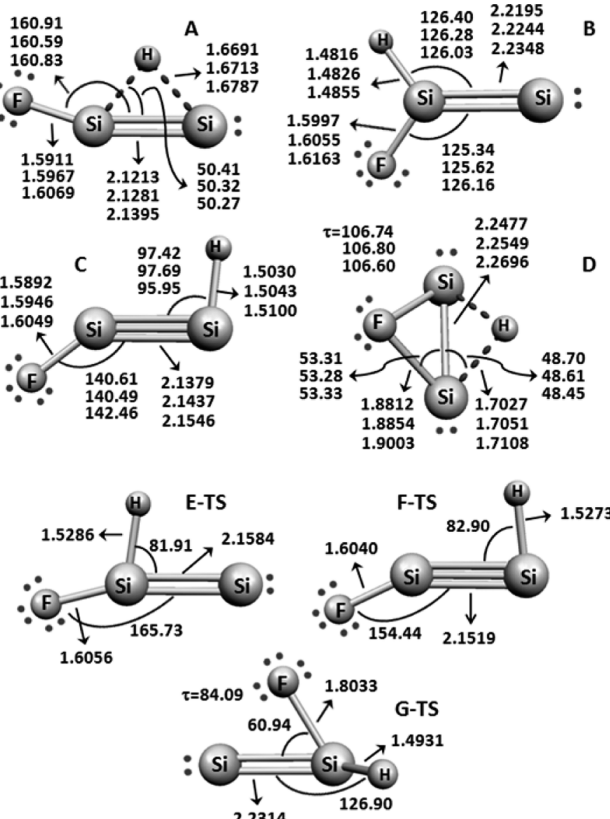


Figure 1. Structures of the Si₂HF minima and transition states. Where three values are shown, the upper one represents the CCSD(T)-F12/VTZ-F12 result, the middle one the CCSD(T)/aVQZ result, and the lower the CCSD(T)/aVTZ result. Single values are the CCSD(T)/aVTZ results. τ is the F–Si–Si–H torsion angle (not shown for planar structures). Distances are in Å, angles in degrees. The bond orders shown were estimated using NBO analysis. Two-electron–three-center bonds are indicated by broken lines. (A) H-bridged minimum. (B) Vinyl minimum (C_s). (C) trans minimum (C_s). (D) Dibridged minimum (C_s). (E) H-bridged/vinyl transition state (C_s). (F) H-bridged/trans transition state (C_s). (G) Vinyl/dibridged transition state (C₁).

triple, or two-electron–three-center bonds shown are those suggested by NBO analysis. In all cases, the proportion of electrons occupying “non-Lewis” orbitals is less than 1% except for trans Si₂HF (1.2%), trans Si₂HCl (1.1%), Si₂HF transition state E (1.3%), Si₂HCl transition state G (1.1%), Si₂HLi Li-bridged (1.2%) and transition state D (1.3%), and Si₂Li₂ dibridged, monobridged, and transition state D (all 1.5%). The energies relative to the respective global minima are displayed in Figures 5–8.

The global minimum for Si₂HF is an H-bridged structure. In addition, vinylidene-like (hereafter referred to as vinyl), trans-bent (trans), and dibridged structures were obtained in order of

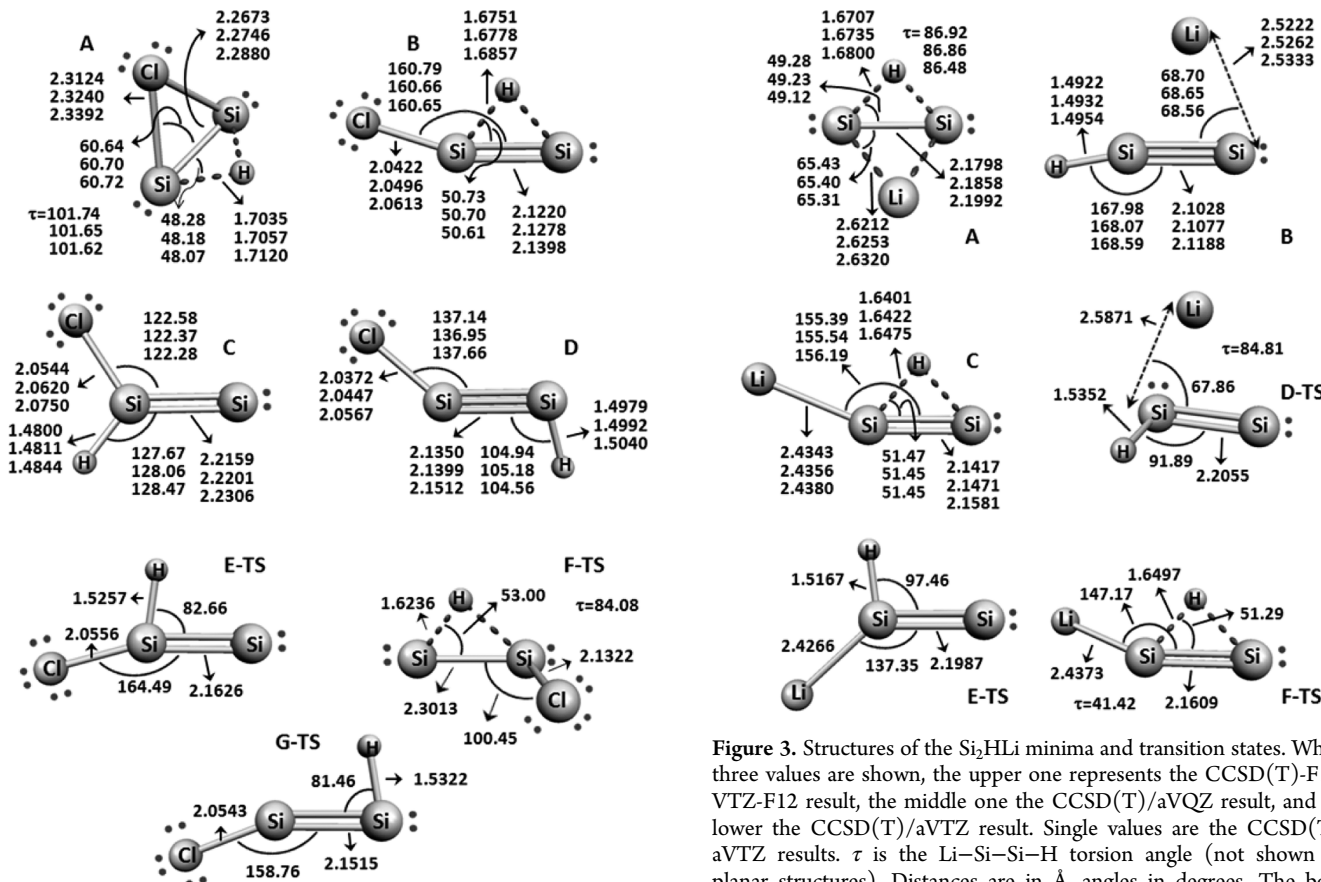


Figure 2. Structures of the Si_2HCl minima and transition states. Where three values are shown, the upper one represents the CCSD(T)-F12/VTZ-F12 result, the middle one the CCSD(T)/aVQZ result, and the lower the CCSD(T)/aVTZ result. Single values are the CCSD(T)/aVTZ results. τ is the $\text{Cl}-\text{Si}-\text{Si}-\text{H}$ torsion angle (not shown for planar structures). Distances are in Å, angles in degrees. The bond orders shown were estimated using NBO analysis. Two-electron–three-center bonds are indicated by broken lines. (A) Dibrigded minimum (C_s). (B) H-bridged minimum (C_s). (C) Vinyl minimum (C_s). (D) trans minimum (C_s). (E) H-bridged/vinyl transition state (C_s). (F) Dibrigded/H-bridged transition state (C_1). (G) H-bridged/trans transition state (C_s).

increasing relative energy. No F-bridged isomer was found (the F-bridged starting structure converged to the vinyl isomer). All Si_2HF minima have C_s symmetry: the H-bridged, vinyl, and trans isomers are planar, whereas the dibrigded isomer possesses a mirror plane through the F and H atoms. The global minima of the other compounds (Si_2HCl , Si_2HLi , and Si_2Li_2) are all dibrigded structures. For Si_2HCl , H-bridged, trans, and vinyl isomers were also found. As for Si_2HF , all four Si_2HCl minima have C_s symmetry (and again the H-bridged, trans, and vinyl isomers are planar). Three bridged Si_2HLi isomers were located: the C_s symmetry dibrigded global minimum and two planar (C_s) monobrigded isomers, one with a bridging H and one with a bridging Li atom. A very shallow trans minimum located on the CCSD(T)/aug-cc-pVTZ potential energy surface of Si_2HLi vanished when other levels of theory were used and was not further considered in this work. Only two Si_2Li_2 minimum-energy structures were located (the C_{2v} symmetry dibrigded global minimum and a planar, C_s symmetry, Li-bridged isomer).

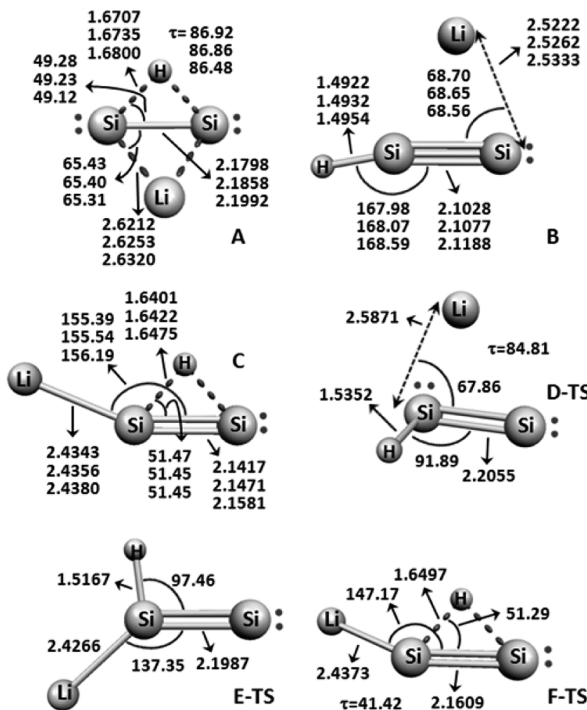


Figure 3. Structures of the Si_2HLi minima and transition states. Where three values are shown, the upper one represents the CCSD(T)-F12/VTZ-F12 result, the middle one the CCSD(T)/aVQZ result, and the lower the CCSD(T)/aVTZ result. Single values are the CCSD(T)/aVTZ results. τ is the $\text{Li}-\text{Si}-\text{Si}-\text{H}$ torsion angle (not shown for planar structures). Distances are in Å, angles in degrees. The bond orders shown were estimated using NBO analysis. Two-electron–three-center bonds are indicated by broken lines. (A) Dibrigded minimum (C_s). (B) Li-bridged minimum (C_s). (C) H-bridged minimum (C_s). (D) Dibrigded/Li-bridged transition state (C_1). (E) Li-bridged/H-bridged transition state (C_s). (F) Dibrigded/H-bridged transition state (C_1).

In addition to the minimum-energy structures, a number of transition states were located on the Si_2HF , Si_2HCl , Si_2HLi , and Si_2Li_2 potential energy surfaces (at the CCSD(T)/aVTZ level). Where necessary, the transition states were confirmed to lie on a reaction path connecting two minima (as indicated in Figures 5–8). For Si_2HF , we located transition states linking the H-bridged and vinyl, H-bridged and trans, and vinyl and dibrigded isomers. The first two are planar and C_s -symmetric, whereas the vinyl/dibrigded transition state does not have any symmetry elements. Note that the (classical) barrier for conversion from the trans to the H-bridged structure is very low (0.11 kcal/mol). Vibrational and temperature effects will be sufficient to surmount this barrier, and thus, the trans structure will likely not be observable experimentally. Also, three Si_2HCl transition state structures were located: one linking the dibrigded and H-bridged minima, one linking the H-bridged and vinyl minima, and one linking the H-bridged and trans minima. The latter two are planar (C_s symmetry), whereas the dibrigded/H-bridged transition state does not have any symmetry elements. All three transition states lie about 12 kcal/mol above the global minimum. However, the barrier for conversion from the trans to the H-bridged isomer is only 0.69 kcal/mol (at the CCSD(T)/aVTZ level). It is therefore unlikely that the trans Si_2HCl isomer can be observed experimentally. Three Si_2HLi transition states were located: one linking the dibrigded and Li-bridged minima, a planar (C_s symmetry) transition state linking

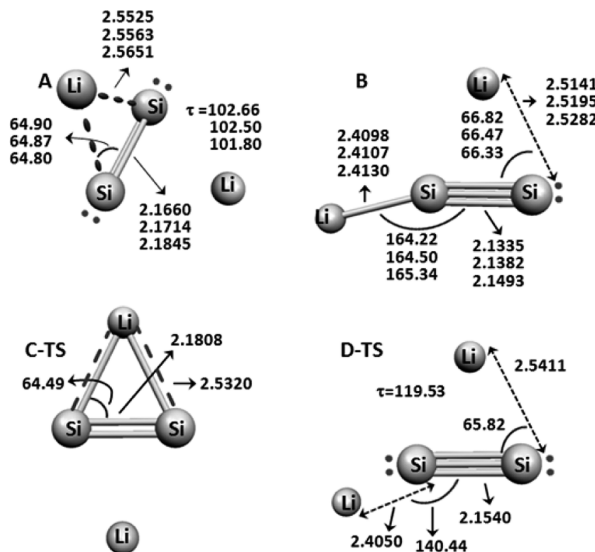


Figure 4. Structures of the Si_2Li_2 minima and transition states. Where three values are shown, the upper one represents the CCSD(T)-F12/VTZ-F12 result, the middle one the CCSD(T)/aVQZ result, and the lower the CCSD(T)/aVTZ result. Single values are the CCSD(T)/aVTZ results. τ is the Li–Si–Si–Li torsion angle (not shown for planar structures). Distances are in Å, angles in degrees. The bond orders shown were estimated using NBO analysis. Two-electron–three-center bonds are indicated by broken lines. (A) Dibridged minimum (C_{2v}). (B) Li-bridged minimum (C_s). (C) Transition state for inversion of dibridged minimum (C_{2h}). (D) Dibridged/Li-bridged transition state (C_1).

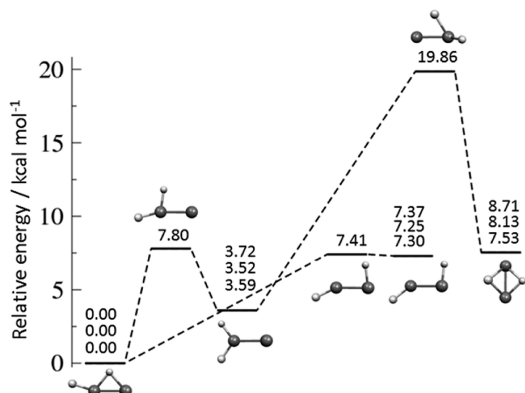


Figure 5. Relative energies (in kcal/mol) for the stationary points of the Si_2HF system. Where three values are shown, the upper one represents the CCSD(T)-F12/VTZ-F12 result, the middle one the CCSD(T)/aVQZ result, and the lower the CCSD(T)/aVTZ result. The corresponding absolute energies for the monobridged isomer are -678.487028 , -678.460251 , and -678.415721 E_h , respectively. Single values are the CCSD(T)/aVTZ results. The dashed lines indicate schematically the associations between transition states and the relevant isomers.

the Li-bridged and H-bridged minima, and one linking the dibridged and H-bridged minima. The barrier for conversion from the H-bridged to dibridged minimum is only 0.02 kcal/mol at the CCSD(T)/aVTZ level. The existence or otherwise of this transition state (and also the H-bridged isomer) should be further investigated using larger basis sets, but it seems clear that any H-bridged isomer is likely not observable. The other barriers for conversion are much higher. Two transition states were located on the Si_2Li_2 potential energy surface: one linking the

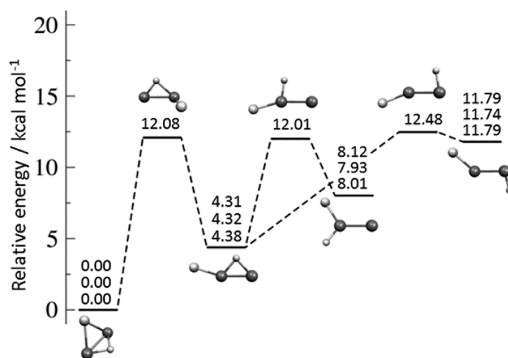


Figure 6. Relative energies (in kcal/mol) for the stationary points of the Si_2HCl system. Where three values are shown, the upper one represents the CCSD(T)-F12/VTZ-F12 result, the middle one the CCSD(T)/aVQZ result, and the lower the CCSD(T)/aVTZ result. The corresponding absolute energies of the dibridged isomer are -1038.472251 , -1038.448039 , and -1038.410561 E_h , respectively. Single values are the CCSD(T)/aVTZ results. The dashed lines indicate schematically the associations between transition states and the relevant isomers.

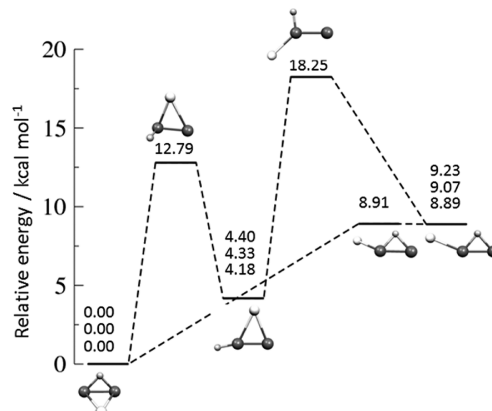


Figure 7. Relative energies (in kcal/mol) for the stationary points of the Si_2HLi system. Where three values are shown, the upper one represents the CCSD(T)-F12/VTZ-F12 result, the middle one the CCSD(T)/aVQZ result, and the lower the CCSD(T)/aVTZ result. The corresponding absolute energies of the dibridged isomer are -586.158123 , -586.146517 , and -586.130456 E_h , respectively. Single values are the CCSD(T)/aVTZ results. The dashed lines indicate schematically the associations between transition states and the relevant isomers.

the two minima located on the potential energy surface (the dibridged and Li-bridged isomers) and a transition state on the inversion path of the dibridged structure. The latter one is planar and has C_{2h} symmetry. The barrier for conversion from the Li-bridged to the dibridged isomer is very low (0.24 kcal/mol), which suggests that the Li-bridged isomer will not be observable.

For Si_2HF and Si_2HCl , the shortest Si–Si bond length occurs in the H-bridged isomers (both 2.14 Å, computed with CCSD(T)/aug-cc-pVTZ). Note that in both cases NBO analysis suggests Lewis structures with Si–Si double bonds. The latter are significantly shorter than those in the corresponding vinyl isomers; the bridging hydrogen in each case increases the overall bonding “between” the silicones. A similar effect is seen in Si_2H_2 ⁴⁶ (where the Si–Si bond lengths for the monobridged and vinyl isomers—determined at the same level of theory⁴—are nearly identical to those of the

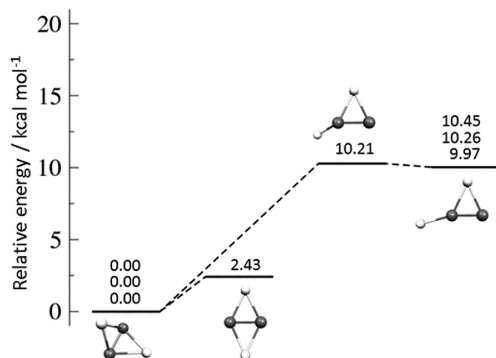


Figure 8. Relative energies (in kcal/mol) for the stationary points of the Si_2Li_2 system. Where three values are shown, the upper one represents the CCSD(T)-F12/VTZ-F12 result, the middle one the CCSD(T)/aVQZ result, and the lower the CCSD(T)/aVTZ result. The corresponding absolute energies are -593.064764 , -593.052849 , and -593.036649 E_h , respectively. Single values are the CCSD(T)/aVTZ results. The dashed lines indicate schematically the associations between transition states and the relevant isomers.

corresponding Si_2HF and Si_2HCl systems). The dibridged isomers have the longest Si–Si bonds (Si_2HF , 2.27 Å; Si_2HCl , 2.29 Å). The NBO analyses suggest single Si–Si bonds, again analogous to the situation in Si_2H_2 .⁴⁶ Note that the nominally triply bonded trans Si_2HF and Si_2HCl isomers have slightly longer bond lengths (both 2.15 Å) than the doubly bonded H-bridged isomers. This apparent anomaly can be rationalized in part by the bridging effect in the latter isomers. However, these “triple” bond lengths are much shorter than might be expected in a linear HSiSiX system analogous to HCCH . (The Si–Si distance in the linear, second-order saddle-point, structure of Si_2H_2 is 2.00 Å at the CCSD(T)/aVTZ level.⁴) In the case of Si_2H_2 , the trans structure (where the Si–Si distance is 2.12 Å at the CCSD(T)/aVTZ level⁴) can be understood as involving relatively weak bent lone-pair donor–acceptor bonds between the notional SiH diatomic fragments.³ The present NBO analyses of Si_2HF and Si_2HCl suggest significantly bent Si–Si bonds also in these cases with natural hybrid orbitals deviating from the lines of centers by 30–60°. All terminal Si–H distances are around 1.5 Å, whereas the Si–H distances in the H-bridged isomers are longer (~1.7 Å). Similarly, the terminal Si–F and Si–Cl distances are shorter (Si–F, 1.6 Å; Si–Cl, 2.1 Å) compared to the corresponding distances in the dibridged isomers (Si–F, 1.9 Å; Si–Cl, 2.2–2.3 Å). For structure G-TS in Figure 1, the Lewis structure shown is that with the lowest non-Lewis fraction, 0.65%. However we also found a similar Lewis structure with only a slightly higher non-Lewis fraction, 0.69%. This one was different in that the Si–F single bond was replaced with a SiFSi two-electron–three-center bond.

For Si_2HLi and Si_2Li_2 , the shortest Si–Si bond length (~2.1 Å) occurs in the Li-bridged structure (where the NBO analyses suggest Si–Si triple bonds); indeed, the Si–Si distance of the Li-bridged Si_2HLi isomer is the shortest among all Si_2HX ($X = \text{F}, \text{Cl}, \text{Li}$) and Si_2Li_2 isomers. The NBO analysis of the dibridged Si_2Li_2 suggests a double Si–Si bond (in contrast to the dibridged isomers of Si_2H_2 , Si_2HF , Si_2HCl , and Si_2HLi where single Si–Si bonds are indicated). In contrast to the H-bridged structures, in the Li-bridged isomers, the terminal H or Li atom is tilted away from the bridging atom. For both Si_2HLi and Si_2Li_2 , the NBO analyses yielded some Lewis structures (B and D-TS in Figure 3 and all in Figure 4) with at least two distinct “molecular units” unconnected by covalent bonds:

$\text{Si}_2\text{H/Li}$, $\text{Si}_2\text{Li/Li}$, or $\text{Si}_2/\text{Li/Li}$. In each case, the natural charge on the noncovalently bonded Li was about +0.7. These results seem consistent with the known significant ionic character of silicon–lithium clusters.¹⁶ In the cases of structures A and C-TS in Figure 4, there are obviously (due to symmetry considerations) equivalent resonance structures with the roles of the Li atoms exchanged. The Si–Si distance in the H-bridged Si_2HLi isomer (2.16 Å) is only slightly larger than that in the corresponding Si_2HF and Si_2HCl isomers. The Si–H distances in Si_2HLi are very close to the corresponding distances in Si_2HF and Si_2HCl (terminal, 1.5 Å; bridged, 1.6–1.7 Å). The Si–Li distances in Si_2HLi and Si_2Li_2 (terminal, 2.4 Å; bridged, 2.5–2.6 Å) are longer than the corresponding Si–F and Si–Cl distances.

On the basis of our Si_2H_2 results (see previous section), the relative energies of the minima obtained with the CCSD(T)-F12/VTZ-F12 method are expected to be the most accurate. In general, the CCSD(T)/aVnZ ($n = \text{T}, \text{Q}$) results agree within 0.6 kcal/mol with the CCSD(T)-F12 values; the only exception concerns the CCSD(T)/aVTZ relative energy of the dibridged Si_2HF isomer, which overestimates the CCSD(T)-F12 result by 1.18 kcal/mol. Thus, to obtain reliable results with CCSD(T), basis sets of at least quadruple- ζ are required.

The minimum-energy structures of the Si_2HCl minima are similar to the corresponding Si_2H_2 isomers and are in the same energetic order. However, their energies (relative to the dibridged structure) are decreased compared to Si_2H_2 . The energies of the Si_2H_2 minima relative to the dibridged global minimum, calculated with CCSD(T)/aVTZ, range from 10.04 kcal/mol (monobridged) to 17.83 kcal/mol (trans),⁴ compared to a range of 4.38 to 11.79 kcal/mol for Si_2HCl . The barriers for conversion of the H-bridged to dibridged and vinyl to H-bridged isomers are larger than those in Si_2H_2 (3.77 and 3.08 kcal/mol, respectively, for Si_2H_2 compared with 7.70 and 4.00 kcal/mol, respectively, for Si_2HCl), whereas the conversion barrier from the trans to the monobridged isomer has decreased from 4.68 kcal/mol (Si_2H_2) to a mere 0.69 kcal/mol. Also for Si_2HF , the same minimum-energy structure types are found as for Si_2H_2 . However, the dibridged structure is now the least stable isomer, with a very large barrier for conversion from the dibridged to the vinyl isomer (12.33 kcal/mol). As for Si_2HCl , the barrier for conversion from the trans to the H-bridged isomer is very low (0.09 kcal/mol). The barrier for conversion from the vinyl to the H-bridged minimum is higher (4.21 kcal/mol) than the corresponding Si_2H_2 barrier (3.08 kcal/mol). The energies relative to the dibridged minimum of the two monobridged Si_2HLi isomers are lower than that of the monobridged Si_2H_2 isomer (Li-bridged Si_2HLi , 4.18 kcal/mol; H-bridged Si_2HLi , 8.89 kcal/mol; monobridged Si_2H_2 , 10.03 kcal/mol). The barrier for conversion from the H-bridged to dibridged Si_2HLi isomer is very much smaller than for Si_2H_2 (Si_2HLi , 0.02 kcal/mol; Si_2H_2 , 3.77 kcal/mol). The relative energy of the monobridged Si_2Li_2 isomer is similar to the corresponding Si_2H_2 isomer, but with a much lower barrier for conversion to the dibridged global minimum (0.24 kcal/mol). The inversion barrier of the dibridged Si_2Li_2 isomer is also much lower (2.43 kcal/mol) than that of the dibridged Si_2H_2 isomer (11.49 kcal/mol).

Bei and Feng optimized different isomers of Si_2HX and Si_2X_2 ($X = \text{F}, \text{Cl}, \text{Br}, \text{Li}$) using Hartree–Fock (HF) theory and the 6-31G** basis set.¹⁵ They did not consider mono- (H or Li) bridged structures and only found planar dibridged structures for Si_2HF , Si_2HCl , and Si_2HLi . This presumably indicates the

failure of the HF method for describing these systems. For Si_2Li_2 , the most stable structure found (based on MP2/6-31G** single-point calculations) was the nonplanar dibridged isomer, in agreement with our results and Boo et al.¹⁶ We are not aware of any higher-level calculations on the Si_2HX ($X = \text{F}, \text{Cl}, \text{Li}$) species. However, several computational studies are available for related Si-containing compounds. Prascher et al.⁴⁷ investigated mixed silicon hydrides and halides ($\text{SiH}_y\text{F}_{x-y}$ and $\text{SiH}_y\text{Cl}_{x-y}$, $x = 1-4$ and $y = 0-x$) at the CCSD(T) level with correlation consistent basis sets up to quintuple-zeta quality. The Si–F distances in SiF_2 , SiHF , and SiH_3F , computed with CCSD(T)/aVQZ, are 1.602, 1.614, and 1.603 Å, respectively, very similar to the CCSD(T)/aVQZ values for the terminal Si–F distances in Si_2HF (trans, 1.5946 Å; H-bridged, 1.5967 Å; vinyl, 1.6055 Å). The CCSD(T)-F12/VTZ-F12 distances are slightly shorter (trans, 1.5892 Å; H-bridged, 1.5911 Å; vinyl, 1.5997 Å). The experimental (equilibrium) bond lengths of SiF_2 , SiHF , and SiH_3F (1.591,⁴⁸ 1.603,⁴⁹ and 1.5945 Å,⁵⁰ respectively) show that the CCSD(T)/aVQZ level overestimates the Si–F bond lengths by about 0.01 Å. Assuming this to be the case for Si_2HF as well, and given that the CCSD(T)-F12/VTZ-F12 level gives bond lengths that are about 0.006 Å shorter than the corresponding CCSD(T)/aVQZ results, this again shows the excellent performance of the CCSD(T)-F12/VTZ-F12 level of theory. Similar comparisons can be made for Si_2HCl and the Cl-containing molecules studied by Prascher et al. The CCSD(T)/aVQZ Si–Cl bond distances for SiCl and SiCl_4 are 2.074 Å and 2.026 Å,⁴⁷ respectively, whereas the experimental bond lengths are about 0.01–0.017 Å shorter (SiCl , 2.057 Å;⁵¹ SiCl_4 , 2.017 Å⁵²). Our results show that the CCSD(T)-F12/VTZ-F12 level of theory gives Si–Cl bond lengths that are 0.007–0.008 Å shorter than the corresponding CCSD(T)/aVQZ values. The CCSD(T)-F12/VTZ-F12 bond lengths are therefore estimated to be very accurate.

Experimental (crystallographic) data exist for molecules containing Si–Li bonds; however, the Si or Li atoms are usually connected to bulky groups like *tert*-butyl. Examples include Si–Li bond lengths in a hydridosilyllithium compound (with bridged Li atoms) of 2.644 and 2.667 Å,⁵³ and Si–Li bond distances for Li in a terminal position of 2.531 Å in tris[di-*tert*-butyl(methyl)silyl]silyllithium⁵⁴ and 2.580 Å in a cyclotrisilanide.⁵⁵ These agree well with our values for bridged Si–Li (ranging from 2.5525 Å in the dibridged Si_2Li_2 isomer to 2.6212 Å in the dibridged Si_2HLi isomer) and for terminal Si–Li (2.4343 Å in the H-bridged Si_2HLi isomer and 2.4098 Å in the Li-bridged Si_2Li_2 isomer), although our results appear to slightly underestimate the experimental bond lengths. We recall that our calculations do not include core correlation, which would further reduce the calculated bond lengths. For Si_2H_2 , core correlation reduces terminal and bridging Si–H distances by ~0.0035 and 0.0045 Å, respectively.⁴ On the other hand, the experimental results are vibrationally averaged distances, which are larger than equilibrium distances. In this case, vibrational averaging and chemical differences may have a larger effect than inclusion of core correlation, which could explain the shorter calculated distances compared to the experimental results. Sporea et al.^{56,57} studied neutral and singly charged mixed silicon–lithium clusters $\text{Si}_x\text{Li}_y^{(+)}$ ($x = 1-6$, $y = 1-2$) employing density functional theory with the B3LYP functional. For Si_2Li_2 , the dibridged structure is reported as the global minimum, followed by the dibridged planar structure and the Li-bridged structure. However, the reported energies⁵⁶ relative to the

global minimum (32.7 and 38.6 kcal/mol, for the planar dibridged and Li-bridged structures, respectively) appear to be too large. Also, the dibridged planar structure is reported⁵⁶ as a minimum; however, our work shows this to be a transition state in agreement with the DFT and MP2 results of Boo et al.¹⁶ The geometries and relative energies reported in the latter work agree reasonably well with our work: at the MP2/cc-pVQZ level, the dibridged isomer Si–Si, Si–Li distances, and Li–Si–Si–Li torsion angle are 2.175 Å, 2.557 Å, and 103.1°, respectively, while the planar transition state Si–Si and Si–Li distances are 2.173 and 2.529 Å, respectively; the energy difference is 2.2 kcal.¹⁶

The harmonic vibrational frequencies, computed at the CCSD(T)/aug-cc-pVTZ level, for the different isomers of Si_2HF , Si_2HCl , Si_2HLi , and Si_2Li_2 are given in Table 3. The

Table 3. Harmonic Frequencies (in cm^{-1}) for the Isomers of Si_2HF , Si_2HCl , Si_2HLi , and Si_2Li_2 , Calculated at the CCSD(T)/aug-cc-pVTZ Level of Theory

	Si_2HF	Si_2HCl	Si_2HLi	Si_2Li_2
dibridged				
	1473.6	1440.7	1495.8	543.0
	969.8	951.3	1180.7	417.4
	839.9	828.3	540.3	403.5
	570.3	501.9	391.9	191.8
	448.5	353.0	316.7	185.0
	166.6	217.7	168.5	107.7
H-bridged				
	1628.2	1624.0	2157.0	610.3
	1053.0	1067.2	592.8	420.1
	920.2	686.0	414.2	419.7
	481.7	389.3	364.4	208.7
	193.6	153.8	237.7	64.4
	118.7	97.0	221.9	44.4
vinyl				
	2222.3	2224.1	1563.7	
	880.1	730.8	1120.1	
	778.7	583.9	606.7	
	472.4	441.6	414.6	
	302.3	278.2	85.8	
	136.7	88.8	34.5	
trans				
	2108.8	2132.0		
	908.1	647.5		
	503.6	472.9		
	423.6	396.0		
	124.8	90.5		
	93.4	49.4		

trans and vinyl isomers of the Si_2HF , Si_2HCl , and the monobridged Si_2HLi isomer each have one frequency with a value above 2100 cm^{-1} . These are due to the SiH stretch modes. In the H-bridged and dibridged isomers of these compounds, the SiH stretch frequencies involving the bridged hydrogen occur at lower frequencies, i.e. between 1400 and 1600 cm^{-1} (symmetric stretch) and 950–1200 cm^{-1} (antisymmetric stretch). Si_2Li_2 , lacking H atoms, does not have such high-frequency modes: the highest-frequency modes in Si_2Li_2 are the SiSi stretches (which in the monobridged isomer is mixed out of phase with the SiLi_t stretch—where Li_t indicates the terminal Li atom). These SiSi stretches occur at 543.0 cm^{-1} for the dibridged and at 610.3 cm^{-1} for the

monobridged isomer. The SiLi stretches in the dibridged Si_2Li_2 isomer occur at rather low frequency (symmetric stretch, 403.5 cm^{-1} ; antisymmetric stretch, 417.4 cm^{-1}). The lowest frequencies are due to out-of-plane vibrations (for example, 44.4 cm^{-1} for monobridged Si_2Li_2 , 34.5 cm^{-1} for H-bridged Si_2HLi , and 49.4 cm^{-1} for trans Si_2HCl). The frequencies determined in the present work for dibridged Si_2Li_2 are $6\text{--}12 \text{ cm}^{-1}$ higher than the DFT values reported by Boo et al.¹⁶ with the exceptions of the SiSi stretch, which is 8 cm^{-1} lower, and the butterfly (τ angle opening) motion (107.7 cm^{-1}), which is 3 cm^{-1} lower.

The range of structures seen above for Si_2HF and Si_2HCl is rather different from C_2HF and C_2HCl , having only the vinylidene-like isomers in common. As was seen in comparing C_2H_2 and Si_2H_2 , the relative energies of the Si_2HF and Si_2HCl isomers are much reduced compared with C_2HF and C_2HCl . None of the Si_2HLi or Si_2Li_2 isomers has an analogue in C_2HLi or C_2Li_2 . On the other hand, the most stable structures of Si_2Li_2 and C_2Li_2 are both dibridged.

4. CONCLUSIONS

The critical points of the substituted disilynes Si_2HF , Si_2HCl , Si_2HLi , and Si_2Li_2 have been investigated using CCSD(T)/aug-cc-pVnZ ($n = T, Q$) and CCSD(T)-F12/cc-pVTZ-F12. In addition, the isomers of Si_2H_2 , for which experimental data are available, were optimized with CCSD(T)/aug-cc-pVnZ and CCSD(T)-F12/cc-pVnZ-F12 ($n = D, T, Q$). The results show the excellent price/performance ratio of CCSD(T)-F12. The geometric parameters computed with CCSD(T)-F12/cc-pVTZ-F12 are of similar or greater quality than the CCSD(T)/cc-pV(5+d)Z results, whereas the CCSD(T)-F12/cc-pVTZ-F12 vibrational frequencies are of comparable accuracy to those computed with CCSD(T)/cc-pV(Q+d)Z. Thus, the CCSD(T)-F12/cc-pVTZ-F12 level of theory manifests itself as a very attractive and cost-effective alternative to conventional CCSD(T).

Dibridged, H-bridged, trans-bent, and vinylidene-like minima were located on the Si_2HF and Si_2HCl potential energy surfaces. However, whereas the Si_2HCl minima are in the same order of stability as the corresponding Si_2H_2 minima (dibridged > H-bridged > vinylidene-like > trans-bent), for Si_2HF the global minimum is the H-bridged structure, and the dibridged minimum is the least favored isomer. Only bridged minima were found for Si_2HLi and Si_2Li_2 : a dibridged and Li-bridged structure for Si_2Li_2 and an additional H-bridged structure for Si_2HLi . For both compounds the dibridged isomer is the global minimum. Si_2HF is therefore the only compound for which the global minimum is H-bridged instead of dibridged. Harmonic vibrational frequencies were calculated at the CCSD(T)/aug-cc-pVTZ level of theory for comparison with possible future experimental IR spectra.

Transition state structures were optimized with CCSD(T)/aug-cc-pVTZ. The resulting barriers indicate that several minima will likely not be observable. These include the Si_2HF and Si_2HCl trans-bent structures, which have very low barriers for conversion to the H-bridged isomer, the H-bridged Si_2HLi isomer (low barrier for conversion to the dibridged minimum), and the Li-bridged Si_2Li_2 structure (low barrier for conversion to the dibridged minimum). The shape of the potential energy surface appears to be very dependent on the particular system. In general, the different isomers are closer in stability, and conversion barriers are mostly lower in the Si_2HX ($X = \text{F}, \text{Cl}, \text{Li}$) and Si_2Li_2 compounds than in Si_2H_2 .

■ ASSOCIATED CONTENT

S Supporting Information

Figures showing the convergence of the bond distances and torsion angle in the dibridged Si_2H_2 isomer with increasing basis set size for CCSD(T) and CCSD(T)-F12 calculations. Figures showing the convergence of the energies of the monobridged vinylidene-like and trans-bent Si_2H_2 isomers (relative to the dibridged global minimum) with increasing basis set size for CCSD(T) and CCSD(T)-F12 calculations. This material is available free of charge via the Internet at <http://pubs.acs.org>.

■ AUTHOR INFORMATION

Corresponding Author

*E-mail: Tanja.vanmourik@st-andrews.ac.uk, m.m.law@abdn.ac.uk.

Present Address

[§]School of Chemistry, University of Nottingham, University Park, Nottingham NG7 2RD, United Kingdom.

Funding Sources

L.M.S. is grateful to the School of Chemistry, University of St. Andrews for a Ph.D. studentship.

Notes

The authors declare no competing financial interest.

■ ACKNOWLEDGMENTS

We thank EaStCHEM for support via the EaStCHEM Research Computing Facility. We are grateful to Kirk Peterson for drawing our attention to the potential of the CCSD(T)-F12 method and the cc-pVnZ-F12 basis sets and to Grant Hill for helpful discussions about F12 basis sets.

■ REFERENCES

- (1) Chang, N.-Y.; Shen, M.-Y.; Yu, C.-H. *J. Chem. Phys.* **1997**, *106*, 3237–3242.
- (2) Grev, R. S.; Schaefer, H. F., III. *J. Chem. Phys.* **1992**, *97*, 7990–7998.
- (3) Lein, M.; Krapp, A.; Frenking, G. *J. Am. Chem. Soc.* **2005**, *127*, 6290–6299.
- (4) Law, M. M.; Fraser-Smith, J. T.; Perotto, C. U. *Phys. Chem. Chem. Phys.* **2012**, *14*, 6922–6936.
- (5) Law, M. M.; Perotto, C. U., *J. Chem. Phys.* Submitted.
- (6) Damrauer, R.; Noble, A. L. *Organometallics* **2008**, *27*, 1707–1715.
- (7) Kuramoto, Y.; Sawai, N.; Fujiwara, Y.; Sumimoto, M.; Nakao, Y.; Sato, H.; Sakaki, S. *Organometallics* **2005**, *24*, 3655–3663.
- (8) Srinivas, G. N.; Schwartz, M. *Inorg. Chim. Acta* **2009**, *362*, 2172–2176.
- (9) Matsumoto, K.; Koshi, M. *J. Electrochem. Soc.* **2008**, *155*, D419–D423.
- (10) Loh, Z.-H.; Field, R. W. *J. Chem. Phys.* **2003**, *118*, 4037–4044.
- (11) DeLeeuw, B. J.; Fermann, J. T.; Xie, Y.; Schaefer, H. F. *J. Am. Chem. Soc.* **1993**, *115*, 1039–1047.
- (12) Riehl, J.-F.; Morokuma, K. *J. Chem. Phys.* **1994**, *100*, 8976–8990.
- (13) Grotjahn, D. B.; Pesch, T. C.; Brewster, M. A.; Ziurys, L. M. *J. Am. Chem. Soc.* **2000**, *122*, 4735–4741.
- (14) Lee, S. Y.; Boo, B. H.; Kang, H. K.; Kang, D.; Judai, K.; Nishijo, J.; Nishi, N. *Chem. Phys. Lett.* **2005**, *411*, 484–491.
- (15) Bei, Y.; Feng, S. *Acta Chim. Sin.* **1999**, *57*, 1306–1312.
- (16) Boo, B. H.; Kim, S.-J.; Lee, M. H.; Nishi, N. *Chem. Phys. Lett.* **2008**, *453*, 150–159.
- (17) Takahashi, M.; Kawazoe, Y. *Organometallics* **2008**, *27*, 4829–4832.
- (18) Borro, A. F.; Mills, I. M. *J. Mol. Struct.* **1994**, *320*, 237–242.

- (19) Holland, J. K.; Newnham, D. A.; Mills, I. M. *Mol. Phys.* **1990**, *70*, 319–330.
- (20) Apponi, A. J.; Brewster, M. A.; Ziurys, L. M. *Chem. Phys. Lett.* **1998**, *298*, 161–169.
- (21) Ihle, M. R.; Wu, C. H.; Miletic, M.; Zmbov, K. F. *Advances in Mass Spectrometry*; Heyden: London, 1976.
- (22) Werner, H. J.; Knowles, P. J.; Knizia, G.; Manby, F. R.; Schütz, M.; Celani, P.; Korona, T.; Lindh, R.; Mitrushenkov, A.; Rauhut, G.; Shamasundar, K. R.; Adler, T. B.; Amos, R. D.; Bernhardsson, A.; Berning, A.; Cooper, D. L.; Deegan, M. J. O.; Dobbyn, A. J.; Eckert, F.; Goll, E.; Hampel, C.; Hesselmann, A.; Hetzer, G.; Hrenar, T.; Jansen, G.; Köpll, C.; Liu, Y.; Lloyd, A. W.; Mata, R. A.; May, A. J.; McNicholas, S. J.; Meyer, W.; Mura, M. E.; Nicklass, A.; O'Neill, D. P.; Palmieri, P.; Pfleiderer, K.; Pitzer, R.; Reiher, M.; Shiozaki, T.; Stoll, H.; Stone, A. J.; Tarroni, R.; Thorsteinsson, T.; Wang, M.; Wolf, A. *MOLPRO*, version 2010.1; Cardiff University: Cardiff, U. K.; Universität Stuttgart: Stuttgart, Germany, 2010.
- (23) Deegan, M. J. O.; Knowles, P. J. *Chem. Phys. Lett.* **1994**, *227*, 321–326.
- (24) Hampel, C.; Peterson, K. A.; Werner, H.-J. *Chem. Phys. Lett.* **1992**, *190*, 1–12.
- (25) Raghavachari, K.; Trucks, G. W.; Pople, J. A.; Head-Gordon, M. *Chem. Phys. Lett.* **1989**, *157*, 479–483.
- (26) Dunning, T. H., Jr. *J. Chem. Phys.* **1989**, *90*, 1007.
- (27) Kendall, R. A.; Dunning, T. H., Jr.; Harrison, R. J. *J. Chem. Phys.* **1992**, *96*, 6796.
- (28) Reed, A. E.; Curtiss, L. A.; Weinhold, F. *Chem. Rev.* **1988**, *88*, 899–926.
- (29) Weinhold, F.; Landis, C. *Valency and Bonding. A Natural Bond Order Donor-Acceptor Perspective*; Cambridge University Press: Cambridge, U. K., 2005.
- (30) Glendening, E. D.; Reed, A. E.; Carpenter, J. E.; Weinhold, F. *NBO*, version 3.1; Theoretical Chemistry Institute, University of Wisconsin: Madison, WI.
- (31) Frisch, M. J.; Trucks, G. W.; Schlegel, H. B.; Scuseria, G. E.; Robb, M. A.; Cheeseman, J. R.; Scalmani, G.; Barone, V.; Mennucci, B.; Petersson, G. A.; Nakatsuji, H.; Caricato, M.; Li, X.; Hratchian, H. P.; Izmaylov, A. F.; Bloino, J.; Zheng, G.; Sonnenberg, J. L.; Hada, M.; Ehara, M.; Toyota, K.; Fukuda, R.; Hasegawa, J.; Ishida, M.; Nakajima, T.; Honda, Y.; Kitao, O.; Nakai, H.; Vreven, T.; Montgomery, J. A., Jr.; Peralta, J. E.; Ogliaro, F.; Bearpark, M.; Heyd, J. J.; Brothers, E.; Kudin, K. N.; Staroverov, V. N.; Kobayashi, R.; Normand, J.; Raghavachari, K.; Rendell, A.; Burant, J. C.; Iyengar, S. S.; Tomasi, J.; Cossi, M.; Rega, N.; Millam, J. M.; Klene, M.; Knox, J. E.; Cross, J. B.; Bakken, V.; Adamo, C.; Jaramillo, J.; Gomperts, R.; Stratmann, R. E.; Yazev, O.; Austin, A. J.; Cammi, R.; Pomelli, C.; Ochterski, J. W.; Martin, R. L.; Morokuma, K.; Zakrzewski, V. G.; Voth, G. A.; Salvador, P.; Dannenberg, J. J.; Dapprich, S.; Daniels, A. D.; Farkas, Ö.; Foresman, J. B.; Ortiz, J. V.; Cioslowski, J.; Fox, D. J. *Gaussian 09*, revision A.02; Gaussian, Inc.: Wallingford, CT, 2009.
- (32) Adler, T. B.; Knizia, G.; Werner, H.-J. *J. Chem. Phys.* **2007**, *127*, 221106.
- (33) Knizia, G.; Adler, T. B.; Werner, H.-J. *J. Chem. Phys.* **2009**, *130*, 054104.
- (34) Hill, J. G.; Peterson, K. A. *Phys. Chem. Chem. Phys.* **2010**, *12*, 10460–10468.
- (35) Peterson, K. A.; Adler, T. B.; Werner, H.-J. *J. Chem. Phys.* **2008**, *128*, 084102.
- (36) Knizia, G.; Adler, T. B.; Werner, H. J. *J. Chem. Phys.* **2009**, *130*, 054104.
- (37) Adler, T. B.; Knizia, G.; Werner, H. J. *J. Chem. Phys.* **2007**, *127*, 221106.
- (38) Yousaf, K. E.; Peterson, K. A. *J. Chem. Phys.* **2008**, *129*, 184108–184107.
- (39) Valeev, E. F. *Chem. Phys. Lett.* **2004**, *395*, 190–195.
- (40) Weigend, F. *Phys. Chem. Chem. Phys.* **2002**, *4*, 4285–4291.
- (41) Weigend, F. *J. Comput. Chem.* **2008**, *29*, 167–175.
- (42) Weigend, F.; Köhn, A.; Hättig, C. *J. Chem. Phys.* **2002**, *116*, 3175–3183.
- (43) Ten-no, S. *Chem. Phys. Lett.* **2004**, *398*, 56–61.
- (44) Bogey, M.; Bolvin, H.; Cordonnier, M.; Demuynck, C.; Destombes, J. L.; Császár, A. G. *J. Chem. Phys.* **1994**, *100*, 8614–8624.
- (45) McCarthy, M. C.; Thaddeus, P. *J. Mol. Spectrosc.* **2003**, *222*, 248–254.
- (46) Chesnut, D. B. *Heteroatom Chem.* **2002**, *13*, 53–62.
- (47) Prascher, B. P.; Luente-Schultz, R. M.; Wilson, A. K. *Chem. Phys.* **2009**, *359*, 1–13.
- (48) Fujitake, M.; Hirota, E. *Spectrochim. Acta A* **1994**, *50A*, 1345–1370.
- (49) Hostutler, D. A.; Clouthier, D. J.; Judge, R. H. *J. Chem. Phys.* **2001**, *114*, 10728–10732.
- (50) Donald, K. J.; Böhm, M. C.; Lindner, H. J. *J. Mol. Struct. (THEOCHEM)* **2005**, *713*, 215–226.
- (51) Mélen, F.; Dubois, I.; Bredohl, H. *J. Mol. Spectrosc.* **1990**, *139*, 361–368.
- (52) Chase, M. W. *J. Chem. Phys. Ref. Data, Monograph* **1998**, *9*, 1–1951.
- (53) Iwamoto, T.; Okita, J.; Kabuto, C.; Kira, M. *J. Am. Chem. Soc.* **2002**, *124*, 11604–11605.
- (54) Nakamoto, M.; Fukawa, T.; Lee, V. Y.; Sekiguchi, A. *J. Am. Chem. Soc.* **2002**, *124*, 15160–15161.
- (55) Abersfelder, K.; Scheschkeiwitz, D. *J. Am. Chem. Soc.* **2008**, *130*, 4114–4121.
- (56) Sporea, C.; Rabilloud, F.; Cosson, X.; Allouche, A. R.; Aubert-Frécon, M. *J. Phys. Chem. A* **2006**, *110*, 6032–6038.
- (57) Sporea, C.; Rabilloud, F.; Aubert-Frécon, M. *J. Mol. Struct. (THEOCHEM)* **2007**, *802*, 85–90.
- (58) Maier, G.; Reisenauer, H. P.; Meudt, A.; Egenolf, H. *Chem. Ber./Recl.* **1997**, *130*, 1043–1046.
- (59) Andrews, L.; Wang, X. *J. Phys. Chem. A* **2002**, *106*, 7696–7702.